Biochemical and Structural Basis for Feedback Inhibition of Mevalonate Kinase and Isoprenoid Metabolism[†,‡]

Zhuji Fu,[||,§] Natalia E. Voynova,[§,△,⊥] Timothy J. Herdendorf,[△] Henry M. Miziorko,*[,△] and Jung-Ja P. Kim*[,||]

Department of Biochemistry, Medical College of Wisconsin, Milwaukee, Wisconsin 53226, Division of Molecular Biology and Biochemistry, University of Missouri—Kansas City, Kansas City, Missouri 64110, and Department of Biochemistry, St. Petersburg State University, St. Petersburg, Russia

Received December 13, 2007

ABSTRACT: Mevalonate kinase (MK), which catalyzes a key reaction in polyisoprenoid and sterol metabolism in many organisms, is subject to feedback regulation by farnesyl diphosphate and related compounds. The structures of human mevalonate kinase and a binary complex of the rat enzyme incubated with farnesyl thiodiphosphate (FSPP) are reported. Significant FSPP hydrolysis occurs under crystallization conditions; this results in detection of farnesyl thiophosphate (FSP) in the structure of the binary complex. Farnesyl thiodiphosphate competes with substrate ATP to produce feedback inhibition of mevalonate kinase. The binding sites for these metabolites overlap, with the phosphate of FSP nearly superimposed on ATP's β-phosphate and FSP's polyisoprenoid chain overlapping ATP's adenosine moiety. Several hydrophobic amino acid side chains are positioned near the polyisoprenoid chain of FSP and their functional significance has been evaluated in mutagenesis experiments with human MK, which exhibits the highest reported sensitivity to feedback inhibition. Results suggest that single and double mutations at T104 and I196 produce a significant inflation of the K_i for FSPP (~40-fold for T104A/I196A). Such an effect persists when K_i values are normalized for effects on the K_m for ATP, suggesting that it may be possible to engineer MK proteins with altered sensitivity to feedback inhibition. Comparison of animal MK protein alignments and structures with those of a MK protein from *Streptococcus pneumoniae* indicates that sequence differences between N- and C-terminal domains correlate with differences in interdomain angles. Bacterial MK proteins exhibit more solvent exposure of feedback inhibitor binding sites and, consequently, weaker binding of these inhibitors.

Mevalonate kinase (MK,[1] EC 2.7.1.36) catalyzes the transfer of the γ-phosphoryl group of ATP to the C5 hydroxyl oxygen of mevalonic acid (*1*). This irreversible reaction requires a divalent cation and represents a key step in the production of polyisoprenoid and sterol metabolites from acetate.

$$\text{mevalonate} + \text{ATP} \rightarrow \text{mevalonate 5-phosphate} + \text{ADP} \quad (1)$$

The importance of the reaction is illustrated by the observation that MK deficiency in humans accounts for the inherited disease mevalonic aciduria (*2*) (MIM 251170). Mevalonate-mediated isoprenoid biosynthesis occurs in animals, invertebrates, plants, fungi, and many bacteria.

Feedback regulation of the pathway has been suggested by early work on pig MK (*3*) and more recent work on recombinant human MK (*4*) which indicates that geranyl diphosphate and farnesyl diphosphate are potent competitive inhibitors with respect to ATP. Other studies on isoprenoid biosynthesis pathway enzymes (*5*) indicate that inhibition by farnesyl diphosphate and geranylgeranyl diphosphate primarily involves mevalonate kinase. Sensitivity to feedback inhibition is much greater for animal (e.g., human) MK (K_i ~ 40 nM) than for bacterial MK (K_i ~ 40 μM) (*6, 7*). It has also been demonstrated that the thiodiphosphate analogue of farnesyl diphosphate (*8*) inhibits MK with a potency similar to that of the physiological metabolite (*6*). *Streptococcus pneumoniae* MK (SpMK) is reported to be inhibited by mevalonate diphosphate (*7*), while the *Staphylococcus aureus* enzyme is not affected by this metabolite (*6*). The biosynthetic pathway to which mevalonate kinase is critical accounts for the production of carotenoids such as zeaxanthin, a target of metabolic engineering which has application in prevention of macular degeneration (*9*). Other downstream pathway metabolites (e.g., farnesyl diphospate, geranylgera-

[†] This work was supported, in part, by NIH Grant DK53766 (H.M.M.) and GM29076 (J.-J. P. K.).

[‡] The atomic coordinates and structure factors have been deposited in the Protein Data Bank (accession codes 2R42 for rMK-FSP and 2R3V for hMK).

* To whom correspondence should be addressed. H.M.M.: Molecular Biology and Biochemistry, University of Missouri—Kansas City, Kansas City, MO 64110; e-mail, miziorkoh@umkc.edu; phone, (816) 235-2246; fax, (816) 235-5595. J.-J.P.K.: Department of Biochemistry, Medical College of Wisconsin, Milwaukee, WI 53226; e-mail, jjkim@mcw.edu; phone, (414) 955-8479; fax, (414) 456-6510.

[||] Medical College of Wisconsin.

[§] These authors contributed equally to this work.

[△] University of Missouri—Kansas City.

[⊥] St. Petersburg State University.

[1] Abbreviations: MK, mevalonate kinase; hMK, human mevalonate kinase; rMK, rat mevalonate kinase; MjMK, *Methanococcus jannaschii* mevalonate kinase; SpMK, *Streptococcus pneumoniae* mevalonate kinase; MVA, mevalonic acid; FPP, farnesyl diphosphate; FSPP, farnesyl thiodiphosphate; FSP, farnesyl thiophosphate; GHMP, galactokinase, homoserine kinase, mevalonate kinase, phosphomevalonate kinase; rms, root-mean-square.

10.1021/bi7024386 CCC: $40.75
Published on Web 02/27/2008

nyl diphosphate, and cholesterol) include polyisoprenoid compounds required for posttranslational modification and onset of function of various proteins important to human development, cellular signaling, etc. Such roles are proposed to account for the inflammatory response associated with the MK deficiency linked to Dutch periodic fever syndrome/hyperimmunoglobulin D syndrome (MIM 260920) (*10*). These observations underscore the physiological importance of feedback control of mevalonate kinase by polyisoprenoid diphosphates.

X-ray structures of animal (*11*) and bacterial (*12*) MK proteins have been published and establish MK as a member of the GHMP kinase family of proteins (*13*). Sensitivity of other members of this protein family to feedback inhibition by polyisoprenoid diphosphates has not been reported. The ATP binding site of MK, for which feedback inhibitors compete, has been clearly indicated only by the structure of the rat MK−ATP binary complex (*11*). Recent publications on the structure of *S. pneumoniae* MK (*14*) and the structure of a putative *Leishmania major* MK (*15*) provide no additional direct experimental evidence for the structure of bound ATP.

To learn more about the nature and efficacy of the feedback inhibition process, we have documented the functional contribution of MK residues situated in the ATP site, which is expected to coincide, at least in part, with the binding site of the competitive feedback inhibitor. To complement such investigation, additional work was aimed at elucidating a three-dimensional structure of a binary complex of animal MK with a feedback inhibitor. We report the structures of human MK and a binary complex of rat MK with farnesyl thiophosphate. The results allow a comparison of ATP and feedback inhibitor binding sites. Similarities as well as functional differences are also illustrated by the characterization of various human MK mutant proteins, which can exhibit different effects on MK interaction with substrate ATP or a feedback inhibitor.

MATERIALS AND METHODS

Escherichia coli JM109 and BL21(DE3) for plasmid propagation and protein expression, respectively, were products of Novagen. Isolation of plasmid DNA was accomplished using Qiagen's miniprep and midiprep kits and protocols. For recombinant protein expression, ampicillin was purchased from Fisher and isopropyl thiogalactoside (IPTG) from Research Products International Corp. Stratagene's Quik-change mutagenesis kit was used for site-directed mutagenesis. Recombinant rat mevalonate kinase was prepared as described by Potter et al. (*16*); recombinant human mevalonate kinase was prepared by the method of Potter and Miziorko (*4*). Farnesyl diphosphate (FPP) was purchased from Echelon Biosciences (Salt Lake City, UT). Farnesyl thiodiphosphate (FSPP) was a generous gift of C. D. Poulter (University of Utah, Salt Lake City, UT). Mevalonic acid was prepared from mevalonolactone as previously described (*16*). Unless otherwise specified, other chemical and biochemical reagents were purchased from Fisher and Sigma, respectively.

Methods. Preparation of Recombinant Wild-Type and Mutant Human Mevalonate Kinase. Human MK was produced in *E. coli*, using a plasmid previously described (*4*). A full-circle PCR method was applied to generate desired mutations. Mutations were produced in human MK (hMK), since it is more sensitive to FPP feedback inhibition than rat MK (rMK). The plasmid pET-3d::HMK was used as a template for PCR. The following forward primers (as well as the corresponding antisense primers) were used to introduce the mutagenic substitution (underlined): L53A, 5′gaaagtggacctcagcgcacccaacattggtatc (TTA changed to GCA); I56A, 5′ggacctcagcttacccaacgctggtatcaagcggg (ATT changed to GCT); T104A, 5′cgactgtgctgtcgccgagcgcctggctg (ACC changed to GCC); Y149A, 5′ctccagcgccgccgcctcggtgtgtctggcag (TAC changed to GCC); I196A, 5′ggggagagaatggctcacgggaacc (ATT changed to GCT); and R388X, 5′ctccctggacagctgagtccagcaagc (CGA changed to TGA).

Double and triple mutants were obtained stepwise, using a plasmid encoding a single mutation as a PCR template and mutagenic primers for the subsequent mutation. The introduction of the desired mutation and the lack of PCR-generated mutations were confirmed by automated DNA sequencing (University of Missouri facility).

Recombinant human MK and mutant forms of the protein were expressed in BL21 DE3 cells. *E. coli* transformants were grown in 0.5 L of LB medium with 100 μg/mL ampicillin at 20 °C. Cells were induced by addition of 1 mM IPTG at an OD_{600} of ~1.2–1.5 and harvested after 12–14 h. Improved expression levels are achieved under these conditions. Cells were suspended in buffer [20 mM phosphate buffer, 1 mM $MgCl_2$, and 0.5 mM DTT (pH 7.5)] supplemented for the lysis step with DNase (final concentration, 1 μg/mL) and phenylmethanesulfonyl fluoride (final concentration, 0.5 mM) and lysed by two passes (18000–22000 psi) through a Microfluidizer cell disruption apparatus. The lysate was centrifuged at 100000*g* for 1 h, and the supernatant was applied on Sepharose Fast Q anion exchange column (50 mL) equilibrated with the same buffer. Enzyme was isolated using a linear gradient (from 20 to 150 mM) of phosphate buffer with 0.5 mM DTT (pH 7.5). The preparations are comparable in homogeneity to the wild-type protein described by Potter and Miziorko (*4*) and are suitable for production of X-ray diffraction quality crystals. Protein was stored in 20% glycerol at −80 °C.

Crystallization and Data Collection. Crystals of hMK were grown at 4 °C using the hanging drop method in 4 μL drops, composed of 2 μL of protein at a concentration of 12 mg/mL in 0.1 M HEPES (pH 7.2) and 2 μL of well solution containing 0.1 M MES (pH 5.6), 18% polyethylene glycol 5000 monomethyl ester (PEG5K MME), 0.1 M NaCl, 1 mM $MgCl_2$, and 0.2 M ammonium sulfate. The crystals were in space group $P2_1$ with the following unit cell dimensions: $a = 102.0$ Å, $b = 78.2$ Å, $c = 109.5$ Å, and $\beta = 113.3°$. Four monomers were found in an asymmetric unit, corresponding to the Mathews coefficient ($V_m = 2.3$ Å^3/Da) and a solvent content of 44.5%.

Crystals of rMK complexed with a feedback inhibitor were obtained from a condition similar to that for hMK crystals, except that the protein solution contained 1 mM FSPP and both the protein and well solutions were buffered with 0.1 M HEPES (pH 7.5). In addition, prior to data collection, the crystals were further soaked in the well solution containing 1 mM FSPP for 2 h. These crystals belong to orthorhombic space group $P2_12_12$ with the following unit cell parameters: $a = 79.0$ Å, $b = 118.4$ Å, and $c = 42.9$ Å. One monomer

Table 1: X-Ray Data Collection and Structure Refinement Statistics

	rMK−FSP	hMK
resolution (Å)	28.03–2.40/2.49–2.40	30.0–2.50/2.59–2.50
no. of collected reflections	34315	149182
no. of unique reflections	13785/882	46210/2397
completeness (%)	84.4/48.3	83.9/44.3
redundancy	2.5/1.7	3.2/2.1
$I/\sigma(I)$	12.2/1.8	17.7/3.2
unit cell dimensions		
a, b, c (Å)	79.0, 118.4, 42.9	102.0, 78.2, 109.5
α, β, γ (deg)	90, 90, 90	90, 113.3, 90
space group	$P2_12_12$	$P2_1$
R_{merge}	0.111/0.327	0.049/0.180
V_m (Å^3/Da)	2.3	2.3
no. of molecules in the asymmetric unit	1	4
	Refinement	
no. of protein atoms	2804	11710
no. of water molecules	73	225
no. of inhibitor atoms	21	
Wilson B (Å^2)	43.0	41.1
average B of main/side chain atoms (Å^2)	51.2/52.7	38.6/40.9
average B of inhibitor atoms (Å^2)	68.4	
average B of water molecules (Å^2)	43.7	37.4
$R_{crystal}$	0.235/0.390	0.234/0.380
R_{free}	0.273/0.380	0.280/0.361
root-mean-square deviation from ideality		
bond lengths (Å)	0.009	0.007
bond angles (deg)	1.40	1.36

was found in an asymmetric unit, corresponding to the V_m value of 2.3 Å^3/Da. Due to difficulties with freezing crystals of both hMK and rMK, data sets for hMK and the rMK−inhibitor complex were collected at 4 °C using an in-house Rigaku R-AXIS IV^{++} detector/MicroMax-007 generator system. In addition, crystals of the rMK−inhibitor complex were extremely radiation sensitive, forcing us to use multiple crystals. Initially, data from five crystals, each with exposure for 4–5 h, were collected. However, in the end, a useable set of data was obtained by merging data from three crystals that gave the best completeness and R_{merge} values. Data collection statistics are given in Table 1. DENZO and SCALEPACK (*17*) were used for data processing.

Structure Determination and Refinement. Since crystals of the rMK−inhibitor complex are isomorphous to those of rMK in complex with ATP (rMK−ATP; PDB entry 1KVK), the structure of the rMK−inhibitor complex was determined by the difference Fourier method. The structure of apo-hMK was determined by the molecular replacement method using MOLREP within the CCP4 program suite (*18*) and the refined coordinates of the rMK−ATP complex (1KVK) without the bound ATP as the search model. For hMK, the initial solution gave four monomers with a correlation coefficient of 0.47 and an R-factor of 0.59 in the resolution range of 20−3.0 Å. After several cycles of refinement, the residues that were not identical between the two enzymes were replaced with the corresponding residues of the human enzyme. The model was manually adjusted to fit the electron density maps using TURBO-FRODO (*19*) on a Silicon Graphics workstation. The FSPP-derived ligand was located from a $F_o - F_c$ difference Fourier map near the ATP binding site. Data collection, processing, and structure refinement statistics are summarized in Table 1.

Kinetic Characterization of Wild-Type and Mutant Human Mevalonate Kinase. Routine enzyme activity measurements were performed spectrophotometrically at 30 °C by using a 0.7 mL mixture [50 mM HEPES (pH 7.5), 100 mM KCl, 10 mM $MgCl_2$, 0.2 mM phosphoenolpyruvate, 0.2 mM NADH, 4 units of lactate dehydrogenase, 4 units of pyruvate kinase, 6 mM ATP, and 1.0 mM (*R*,*S*)-mevalonic acid]. Activity was calculated by using the extinction coefficient for NADH at 340 nm (6.22 cm^{-1} mM^{-1}). Protein concentration was measured by the Bradford assay by using bovine serum albumin as the standard. For determination of K_{mATP}, ATP concentrations were varied from 0.02 to 6 mM at saturating concentrations of mevalonic acid (1–7 mM, depending on mutant affinity). Variable concentrations of (*R*,*S*)-mevalonic acid (from 0.017 to 3.5 mM) at a fixed saturating concentration of ATP (6 mM) were used to determine V_{max} and K_m values for (*R*,*S*)-mevalonic acid. In experiments on FPP inhibition, concentrations between $0.5K_i$ and $11K_i$ were used. To determine steady-state kinetic parameters, data were subjected to nonlinear regression fits to the Michaelis–Menten equation using Grafit (Erithacus Software). To determine K_i for FPP (a linear competitive inhibitor with respect to ATP), the same program was used for multicurve fits.

RESULTS

Description of the Rat MK Protein Structures. The overall structure of rMK is essentially the same whether ATP or FSPP derivative is bound to the enzyme, with an rms deviation of 0.42 Å between the two binary complex structures. The monomer fold of the dimeric molecule consists of two tightly associated domains, the larger N-terminal and slightly smaller C-terminal domains (Figure 1). As in the structure of the rMK−ATP complex (*11*), residues between positions 75 and 85 could not be located. In addition, densities for the side chains of residues 86−105 were also not well defined, and therefore, they were modeled as alanines (except, when indicated, for residue 104).

Although FSPP was present in the crystallization medium, the β-PO_4 of the inhibitor could not be fitted to the experimental electron density, while the rest of the FSPP molecule, including the farnesyl chain and the α-PO_4, was clearly seen (Figure 2). Therefore, FSP, instead of FSPP, was modeled in the density. The observation of bound FSP was surprising and could reflect either disorder or cleavage of the β-phosphate of FSPP used during crystallization. To independently test the possibility of hydrolysis, the enzyme was incubated in the same buffer (without precipitant) used for crystallization and at a comparable ratio (~4:1) of FSPP to protein sites. Inorganic phosphate measurements indicated hydrolysis of 33% of the inhibitor's β-phosphate within 4 days (less time than the time at which protein crystals were harvested). Negligible levels of phosphate (~2%) were produced from FSPP upon incubation in the absence of enzyme. Thus, a slow, nonphysiological enzyme-catalyzed reaction may explain the detection of FSP in the structure of the rat MK−inhibitor complex.

FIGURE 1: Overlay of structures of human MK (green), the rat MK−FSP binary complex (gray), and the rat MK−ATP complex (magenta). N- and C-termini are marked. The disordered regions in all three structures are marked with dotted lines: residues 76–79 in human MK, 75–85 in the rat MK−FSP complex, and 73–88 in the rat MK−ATP complex. FSP and ATP are shown with balls and sticks in atom colors and magenta, respectively. Figures 1−4 were generated using Molscript (*30*) and Raster3D (*31*).

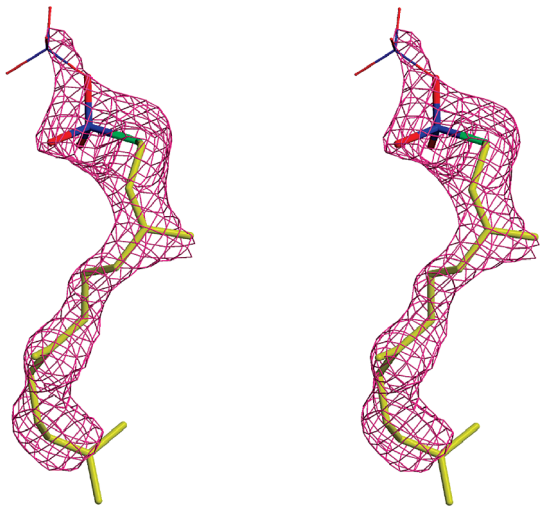

FIGURE 2: Stereodiagram of a model of Mg-FSP fitted into an omit $|F_o| - |F_c|$ map. The map is contoured at 2.5σ. The sulfur atom is colored green. There is a hint of density for the β-PO_4 (estimated occupancy, ~10–20%) of the bound inhibitor, which is shown with thin sticks in Figures 2, 3, and 6.

The inhibitor binds at the cleft between the two domains of the enzyme molecule, at the same location where ATP binds in the structure of the rMK−ATP complex, with the PO_4 of FSP nearly superimposing on the β-PO_4 of ATP, and the polyisoprene tail overlapping the ATP adenine moiety. Interestingly, side chain conformations that are well-defined

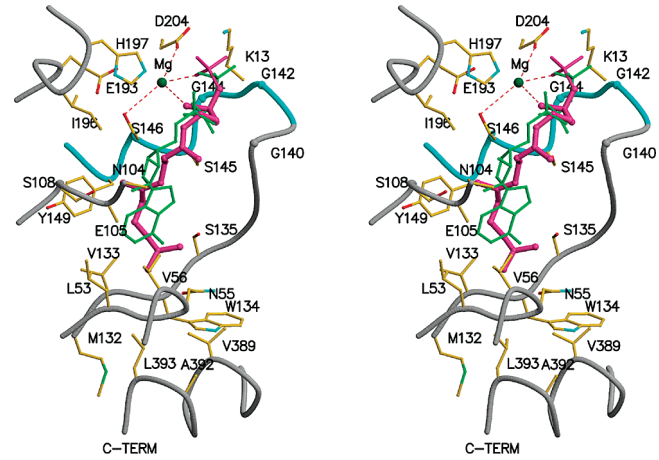

FIGURE 3: Stereodiagram of the vicinity of the ligand binding site in rat MK. The feedback inhibitor, farnesyl thiodiphosphate, is represented by thick magenta sticks. The Mg^{2+} ion (dark green ball) coordinates to D204, S146, and the phosphate oxygen atom of FSP. For comparison, ATP (green sticks) found in the rat MK−ATP binary structure is overlaid showing that both ligands bind at the same site of the MK protein. The motif 2 loop (cyan tubing) of the MK polypeptide wraps around the phosphate of FSP or the β- and γ-phosphate of ATP. Note that the α-phosphate and low-occupancy β-phosphate groups of FSPP correspond to β- and γ-phosphates of ATP, respectively. Side chains of I196 and N104 are within 6 Å of the second isoprenyl group; V133 and the side chains of the loop containing L53, N54, and V56 make hydrophobic interactions with the third isoprenyl group. The latter loop is absent in *S. pneumoniae* MK.

FIGURE 4: Structural comparison of animal MK and bacterial MK. Structures of human MK (green) and SpMK (purple) are overlaid using only their N-terminal domains superimposed. Bound ligands are shown with balls and sticks: FSP of human MK in atom colors and diphosphomevalonate bound to SpMK colored blue. The N- and C-terminal domains in human MK stack straight on top of each other (interdomain angle, ~180°; the interdomain angle is arbitrarily defined as the angle between the plane of the β-sheet in the N-terminal domain and the axis of helix 10 in the C-terminal domain), whereas the corresponding angle in SpMK is bent by 30° (interdomain angle, ~150°).

for some residues lining the FPP/ATP-binding pocket remain unchanged, except that Ser108, which makes a hydrogen bond with the 2′-OH group of the ATP ribose, is flipped away from the ligand in the structure of the rMK−FSPP complex.

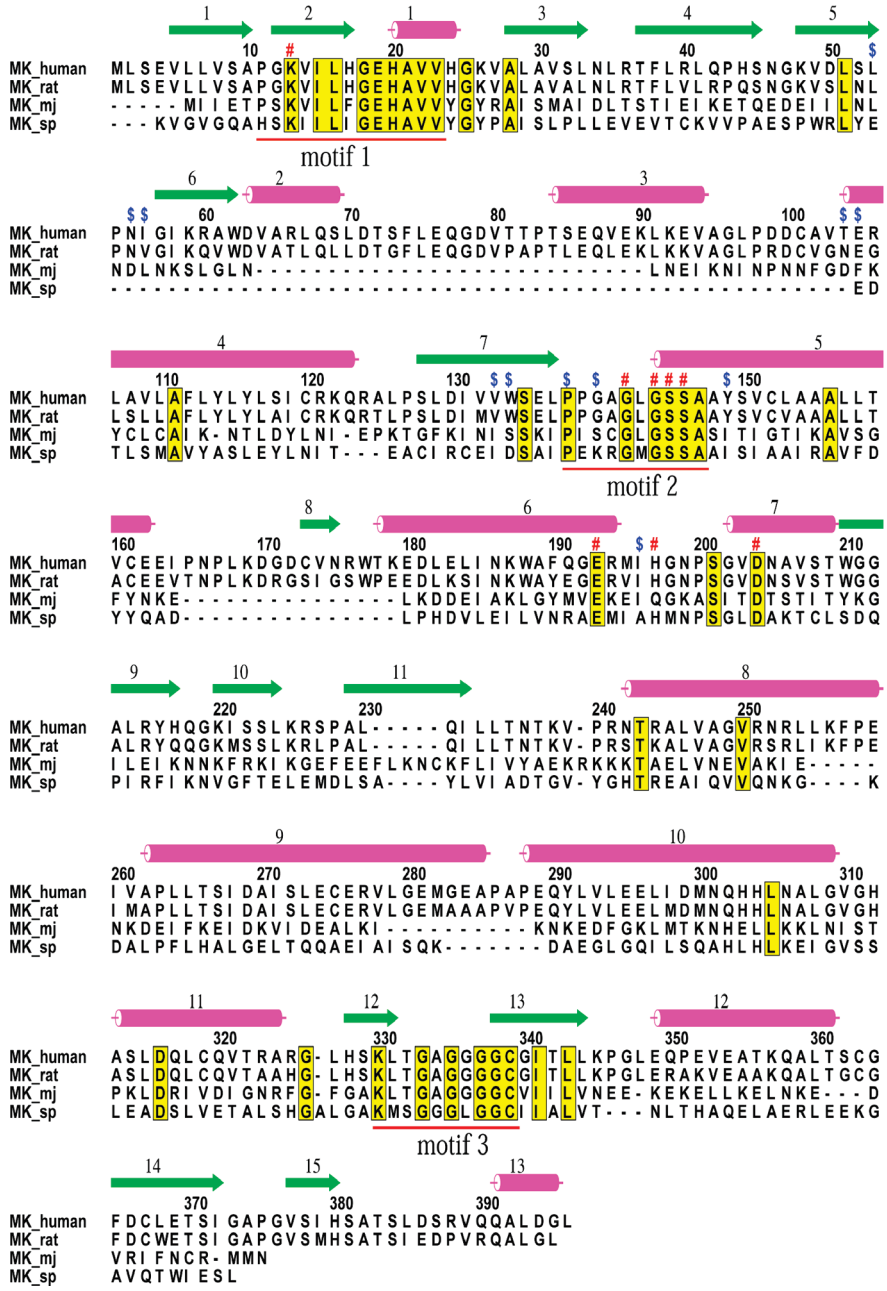

FIGURE 5: Structure-based sequence alignment of animal and bacterial MK proteins. Strands and helices are depicted with green arrows and red cylinders, respectively. Conserved residues in all four proteins are highlighted in yellow. Residues involved in binding of the phosphate portion of FSP (or ATP) are marked with red number signs, and those involved in the isoprenoid moiety binding are denoted with blue dollar signs. Three conserved GHMP motifs are marked and underlined in red. This figure was generated using Alscript (*32*).

Structure of Human MK. As expected from the sequence similarity (81.8% identical), the structure of hMK is the same as that of rMK, with an rms deviation of 0.81 Å (for 372 Cα atoms), whereas among the four monomers of hMK in the asymmetric unit, the rmsd range is 0.69−0.84 Å. Since the structure of rMK does not change upon binding to ATP or FSPP, it can be assumed that the hMK structure remains the same when it binds to FSPP. Therefore, the structure of the hMK−FSP complex can be easily modeled by overlaying the structures of apo-hMK and the rMK−FSP complex, i.e., by modeling the structure of the hMK−FSP complex after that of the rMK−FSP complex.

Feedback Inhibitor Binding Site. Figure 3 shows the vicinity of the FSPP binding site in the structure of the rMK−FSP complex. As in the case of ATP binding, the glycine-rich motif 2 loop [^{138}PPGAGLGSSA^{147} (Figure 3)] wraps around the phosphate moiety of FSP. These interactions between the phosphate of FSP and the protein are mostly conserved in the rMK−ATP structure with β-PO_4 of ATP replacing the phosphate of FSP. The polyprenyl tail is surrounded mainly by hydrophobic residues, I196, the phenyl ring of Y149, and N104 (T104 in hMK). The "bottom" of the binding pocket where the third isoprenyl group binds is lined with L53, N55, V56, and V133. The pocket is not very deep but wide enough to accommodate binding of geranylgeranyl diphosphate. The excess volume of the pocket unoccupied by FSP calculated using CASTp (*20*) is ~103 Å^3, which is just enough for one additional isoprene group. This is consistent with the results of the inhibition studies in which the degree of inhibition is very similar between C15 and C20 prenyl carbon chains (*5*).

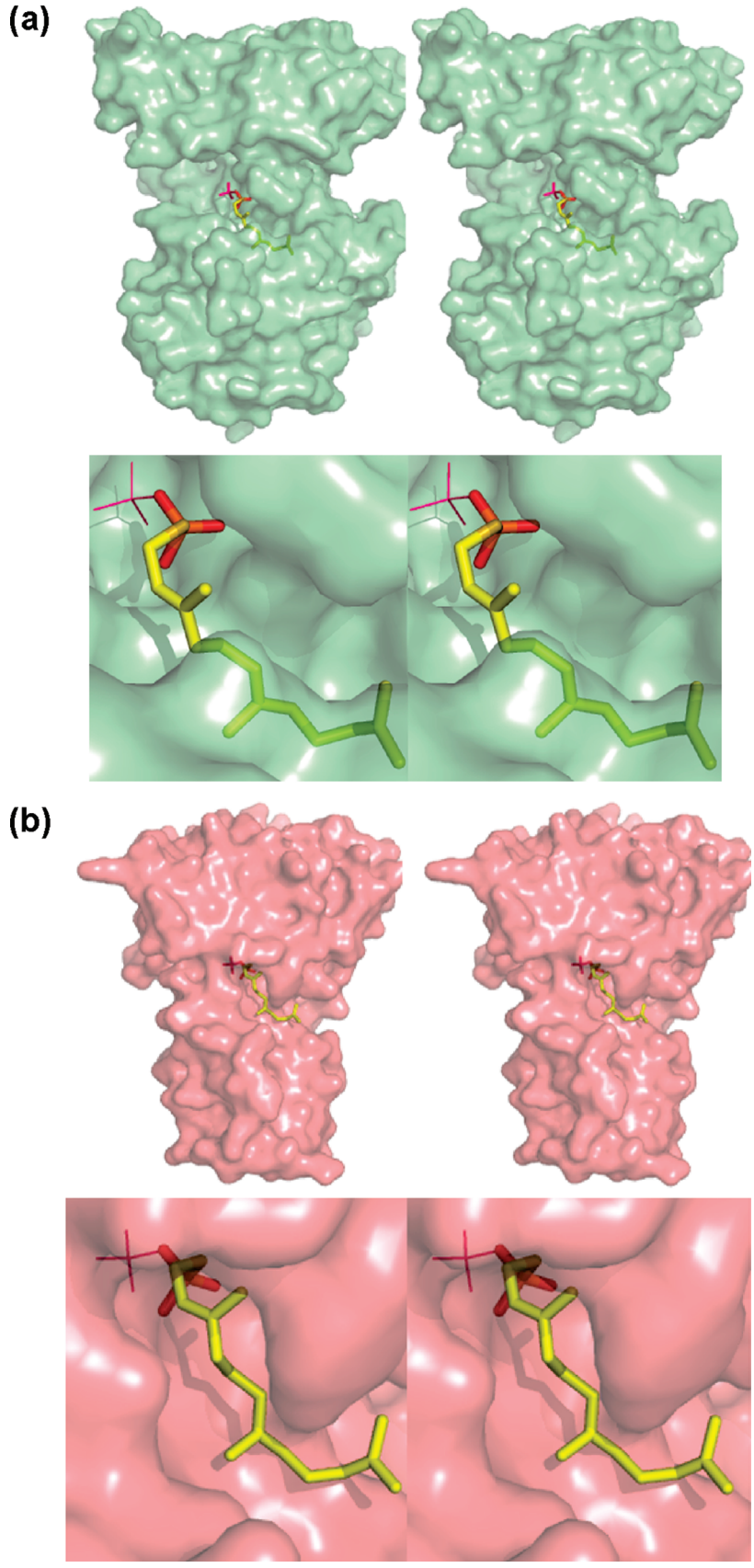

FIGURE 6: Comparison of the substrate ATP or feedback inhibitor binding sites for human and bacterial MK proteins. Stereoviews of the solvent-accessible surfaces of the inhibitor binding site of human MK (a) and SpMK (b). The FSPP molecules in both human and Sp MKs are modeled after the structure of the rat MK−FSP binary complex. The top panels show the entire monomer structures, and the bottom panels are enlarged views of the inhibitor binding sites. (a) The second and third isoprenoid groups in human MK are completely embedded by side chains of I196, T104, L53, N54, and I56. (b) The isoprenoid portion of the modeled FSPP in the SpMK structure is completely exposed to the solvent due to the lack of residues 55–104 (human MK numbering; see Figure 5), while the diphosphate moiety is more shielded than that in human MK. Figures were produced using PyMol (*33*).

Strategy for Mutagenesis of Human Mevalonate Kinase. Structures of the ATP and FPP binding sites in binary complexes of MK with ATP or farnesyl thiophosphate (FSP) were examined for residues with hydrophobic moieties that might be responsible for stabilizing interactions with the branched carbon chain of the farnesyl moiety. Some structural ambiguity in the protein backbone and several side chains that are in the proximity of the farnesyl moiety added to the importance of the production and solution-state characterization of mutant MK proteins. Mutations were produced using human MK, since it is more sensitive to FPP inhibition than rat MK. "In silico" replacement of target amino acids in the structures of the human enzyme or the rat binary complexes with a proposed mutant residue was performed using the Swiss "Deep View" mutation tool, further guiding decisions about mutation sites. Residues within reasonable distance for hydrophobic interaction were considered for mutagenesis. These include amino acids with a side chain orientation toward the ATP-binding pocket of the enzyme cleft. Other considerations included residues that could possibly interact with other hydrophobic amino acids, since a cluster of hydrophobic residues might affect the binding of FPP. Alanine substitution was designed to minimize side chain interactions with substrate or inhibitor and, in some cases, to minimize disruption of β-strand structure.

In addition to these single-residue mutations, since *St. aureus* MK shows low sensitivity to FPP inhibition (*6*) and lacks the C-terminal helix that is adjacent to the ATP/FPP binding cleft in the more sensitive animal enzymes, a truncated form of human MK (R388X) was produced. This truncation also has potential physiological significance since a human MK R388X mutation has been implicated in a deficiency of this enzyme associated with hyperimmunoglobulin D syndrome (*21*) but has not been characterized. This truncated protein was also investigated as a platform for mutations in experiments that complement studies performed using full-length human MK.

Kinetic Characterization of Human Mevalonate Kinase Mutant Proteins. On the basis of the structure of the binding sites for ATP and farnesyl thiophosphate in rat mevalonate kinase, side chains of several residues (e.g., L53, I/V56, T/N104, Y149, and I196) that appear to interact with bound substrate or inhibitor were mutated in human MK, which exhibits a higher affinity for feedback inhibitor than does rat MK (*6*). A double mutant (T104A/I196A) was also isolated and characterized after single mutants had been initially characterized. Additionally, truncated MK R388X protein was characterized since the *St. aureus* protein lacks this region and exhibits weaker binding of the feedback inhibitor (*6*). None of the residues mutated had previously been tested for function (including the inherited mutation R388X), and they are not in the proximity of residues (e.g., K13, S146, and D204) previously implicated in catalytic function (*4, 16, 22*). For this reason, it is not unexpected that these mutants exhibit only modest changes in V_m in comparison with the wild-type human MK value (Table 2). An inflation of the mevalonate K_m is most notable for Y149A (~8-fold) and for the double mutant in the truncated protein (T104A/I196A/R388X, ~11-fold). Since the phosphoryl acceptor substrate, mevalonate, must be positioned adjacent to the γ-phosphoryl of ATP, observation of only modest effects on K_m for mevalonate seem reasonable for mutations that are not near the phosphoryl chain. These mutants also exhibit only modest inflations of K_m for ATP, with the largest effect (~4.5-fold) measured for I56A (Table 2). Documentation of these effects on ATP affinity becomes more useful when they are normalized to effects on mutant sensitivity to MK feedback inhibition.

Table 2: Kinetic Characterization of Human MK Mutants[a]

enzyme	V_m (units/mg)	K_{mMVA} (μM)	K_{mATP} (μM)
wild type	28.0 ± 1.6	40.8 ± 0.7	178.4 ± 18.7
L53A	20.5 ± 1.4	47.3 ± 13.0	232.1 ± 31.7
I56A	28.3 ± 0.9	228.2 ± 2.1	809.7 ± 68.7
Y149A	17.1 ± 0.2	323.2 ± 8.3	689.6 ± 61.7
T104A	23.2 ± 0.4	32.4 ± 2.3	40.3 ± 4.8
I196A	21.2 ± 0.8	116.3 ± 1.4	301.8 ± 28.7
T104A/I196A	23.8 ± 1.1	74.5 ± 1.6	307.7 ± 40.8
T104A/I196A/R388X	23.5 ± 1.3	459.1 ± 63.8	395.4 ± 28.1
R388X	47.0 ± 2.1	45.9 ± 8.2	614.0 ± 93.0

[a] For determination of K_{mATP}, a range of ATP concentrations from 0.02 to 6.0 mM was employed at a fixed saturating concentration of mevalonic acid (1–7 mM, depending on mutant affinity). For determination of V_m and K_{mMVA}, mevalonic acid concentrations from 0.017 to 3.5 mM were employed at a fixed saturating concentration of ATP (6 mM). Activity measurements were performed at 30 °C.

Feedback Inhibition of Human Mevalonate Kinase Mutant Proteins. While all mutated residues map within the binding site for ATP and farnesyl diphosphate, it seemed that human MK T104 and I196 residues could interact significantly with the branched chain farnesyl moiety. On the basis of the inflation of the K_i for farnesyl diphosphate initially observed upon mutation of these residues (Table 3), double mutants were produced in full-length (T104A/I196A) and truncated MK (T104A/I196A/R388X) and characterized. These double mutants exhibit notable K_i inflation effects (~39- and ~50-fold, respectively). These observations implicate the side chains which are missing in the mutant residues in a potentially cooperative effect on binding of the feedback inhibitor, FPP (Table 3).

When the K_i ratios for mutant versus wild-type human MK proteins are normalized for effects on K_m for ATP, the most notable effects are observed for changes at residues T104 and I196, in contrast with values for residues L53, I56, and Y149 (Table 3). Data for double mutants (T104A/I196A and T104A/I196A in R388X; ~23-fold effects) reflect the largest changes and underscore the significance of effects observed on the K_i for FPP. The combined data indicate that, despite the partial overlap in ATP and FPP binding sites, differences in particular interactions and side chain contributions influence binding of adenosyl and farnesyl moieties and suggest that it might be possible to engineer a MK protein with altered affinity properties and sensitivity to feedback inhibition by downstream metabolites.

Structural Comparison of Animal MK with Bacterial MK. The crystal structure of *S. pneumoniae* MK (SpMK) in complex with diphosphomevalonate has been reported recently (*14*). Although its overall fold is the same as that of the animal MKs, the interdomain angle in SpMK is different from those of animal MKs (Figure 4). While the two domains in the animal (rat and human) MK structures stack well on top of each other (i.e., interdomain angle of 180°), the corresponding angle observed upon overlay of bacterial MK proteins on animal MK proteins is 150° for SpMK and 165° for MjMK. This contrast, which is probably

Table 3: Farnesyl Diphosphate (FPP) Feedback Inhibition of Human MK Mutants

enzyme[a]	K_{iFPP}[b] (nM)	K_{iFPP} mutant/ wild-type ratio	K_{mATP} (μM)	K_{mATP} mutant/ wild-type ratio	K_{iFPP} ratio/ K_{mATP} ratio
wild type	34.0 ± 5.0	1.0	178.4 ± 18.7	1.0	1.0
L53A	73.4 ± 12.8	2.2	232.1 ± 31.7	1.3	1.66
I56A	55.3 ± 4.9	1.6	809.7 ± 68.7	4.5	0.36
Y149A	62.6 ± 5.2	1.8	689.6 ± 61.7	3.9	0.46
T104A	74.9 ± 10.9	2.2	40.3 ± 4.8	0.2	11.0
I196A	180.7 ± 16.8	5.3	301.8 ± 28.7	1.7	3.12
T104A/I196A	1313 ± 147	38.6	307.7 ± 40.8	1.7	22.7
T104A/I196A/R388X	1713 ± 150	50.4	395.4 ± 28.1	2.2	22.9
R388X	85.7 ± 11.1	2.5	614.0 ± 93.0	3.4	0.74

[a] For several mutated human MK residues located in the central or distal part of the inhibitor binding pocket, the closest distances between the corresponding side chains and bound inhibitor in the structure of the rat MK−FSP complex are as follows: from L53 to C11[1], 3.6 Å; from I56 to C11[1], 4.1 Å; from T/N104 to C3[1], 5.0 Å; from I196 to C7[1], 6.0 Å. Distance estimates from the observed rMK−FSP structure are slightly larger than expected for tight van der Waals interactions. They are compatible with the hMK mutagenesis results [values for ATP-normalized FPP binding effects (K_{iFPP}/K_{mATP})] since, due to several factors, they may only approximately reflect only the hMK−inhibitor site. There is some structural ambiguity for the side chains of residues 86–105 (including T/N104). A slight (0.8 Å) rms deviation is calculated between α-carbons of the rMK and hMK structures. There also is an assumption of no structural changes in hMK upon inhibitor binding. [b] K_i values for farnesyl diphosphate (FPP), a linear competitive inhibitor with respect to ATP, were determined at saturating concentrations of mevalonic acid (from 1.3 to 7 mM, depending on mutant affinity). ATP concentrations ranged from 0.02 to 6 mM, in the presence of different fixed concentrations of farnesyl diphosphate (from 0.5K_i to 11K_i). Measurements were taken at 30 °C.

due to the lack of 50 residues in SpMK and ~25 residues in MjMK, allows the two domains to bend together. This extra region is present only in the animal MK [residues 53–104 (Figure 5)]. It constitutes part of the FPP binding pocket, thereby facilitating the isoprenoid binding in animal MK. In the bacterial MK structure, the binding pocket for the farnesyl moiety of FPP is rather exposed to the solvent (Figure 6), accounting for weaker binding of the polyprenyl moiety and the low sensitivity [no effect at 14 μM (*7*)] to feedback inhibition by FPP.

DISCUSSION

The secondary structure of human and rat mevalonate kinase proteins, including the ATP/feedback inhibitor sites, includes a mixture of α-helices and β-strands; these proteins tightly bind farnesyl diphosphate (human MK $K_{iFPP} \sim 34$ nM). In contrast, many other farnesyl diphosphate-binding proteins are characterized by a largely α-helical secondary structure and a hydrophobic α-barrel provides interactions with the polyisoprenoid chain. These include protein farnesyl transferase (*23*), avian prenyl transferase/farnesyl diphosphate synthase (*24*), and a variety of terpenoid synthases, including pentalenene synthase (*25*) and aristolochene synthase (*26*). On the basis of our observations for human and rat MK proteins, the hydrophobic interactions that support nucleotide substrate binding also enhance binding of the hydrophobic feedback inhibitor, farnesyl diphosphate.

For *S. pneumoniae* MK (*14*), although no bound ATP was detected, a more solvent-accessible ATP binding site has been hypothesized. Such an environment may account for the failure to observe significant farnesyl diphosphate inhibition of this enzyme (no inhibitory effect reported at a concentration of 14 μM) (*7*). Much weaker FPP affinity is associated with bacterial MK proteins that lack stretches of amino acids in the N-terminal domain or lobe of the protein; these proteins also exhibit different interdomain angles in comparison with the animal MK proteins. For the bacterial MK proteins, these factors can contribute to a more open groove and/or fewer hydrophobic contacts in their putative ATP/FPP binding sites (Figure 6b) and would explain the consequent inefficiency in feedback inhibition by FPP in comparison with animal MK proteins.

Mevalonate kinase proteins are inhibited both by farnesyl diphosphate and by farnesyl thiodiphosphate. The latter compound has been particularly useful in forming a binary FSP complex with rat MK that survives crystallization. While inhibition by these compounds is competitive with respect to ATP, K_{iFPP} values for human and bacterial enzymes differ by 1000-fold (*6*) but K_{mATP} values differ by only 2–4-fold. This observation suggests that, while the phosphates of FPP or FSPP may compete for the binding site of the phosphoryl groups of ATP [as demonstrated by the MK−FSP structure (Figure 3)], large contributions to inhibitor affinity are derived from binding interactions for the farnesyl and adenosyl moieties. Aliphatic residues and relatively few aromatic side chains are involved in many of these binding interactions.

Inhibition of pig MK (*3*) by geranyl diphosphate and the recombinant human enzyme (*6*) (82% identical in sequence with rat enzyme) by farnesyl diphosphate has been reported. Both mevalonate kinase (*11, 12*) and mevalonate diphosphate decarboxylase (*27*) exhibit similar protein folds. A study that employed GST fusions of these proteins (*5*) tested the specificity of their inhibition by prenyl diphosphates and indicated that mevalonate kinase, but not mevalonate diphosphate decarboxylase, was particularly sensitive. Geranyl, farnesyl, and geranylgeranyl diphosphate exhibit significant efficacy of inhibition ($K_i \sim$ 59–116 nM) that changes little in magnitude between inhibitors with $C_{10}-C_{20}$ prenyl carbon chains. In contrast, C_5 isopentenyl or dimethylallyl diphosphates are much weaker inhibitors ($K_i \sim$ 16–20 μM). Thus, feedback inhibition of polyisoprenoid and sterol biosynthesis in animals is primarily attributable to mevalonate kinase effects by long chain prenyl diphosphates. Interactions between enzyme residues in the middle of the binding pocket (e.g., I196, T/N104) and the adjacent C_5 isoprenoid units contribute substantially to inhibitor binding. Some residues located more distally in the binding cleft (e.g., Y149, I/V56) may have a stronger influence on affinity for nucleotide substrate than for farnesyl diphosphate. Others such as L53 make a modest contribution to FPP affinity. Experimental results from kinetic characterization of alanine mutants of human MK do not support any a

priori prediction that the hydrophobic patch of residues at the distal end of the FPP pocket might make a dominant contribution to FPP versus ATP binding. This may be important if the enzyme is to accommodate longer prenyl chain inhibitors. Instead, the mutagenesis data indicate that the contributions and contacts of multiple residues (including ones in the middle of the prenyl pocket) provide synergy in FPP binding and account for the affinity of FPP at the nucleotide substrate/feedback inhibitor site of animal MK proteins.

The ability of FPP to influence metabolism may be more widespread than previously appreciated. FPP and other isoprenoid diphosphates bind to methyl-erythritol-2,4-cyclodiphosphate synthase (*28, 29*), an enzyme in an alternative pathway for isoprenoid biosynthesis. Structural studies on the *Shewanella oneidensis* and *E. coli* enzymes indicate that binding occurs not at the catalytic site but in a hydrophobic cavity formed by the trimeric enzyme. The physiological significance of these interesting observations remains to be explored. However, it does seem clear that, in the mevalonate-mediated pathway for polyisoprenoid biosynthesis, relief of MK feedback inhibition could improve the yield of complex lipids or natural products from metabolically engineered organisms. Also, inherited diseases that involve mevalonate kinase deficiencies might be ameliorated by minimizing feedback inhibition that diminishes production of polyisoprenoids from a mevalonate precursor. Polyisoprenoid modification of proteins is now recognized as an important posttranslational process with implications for developmental biology, inflammatory diseases, and cancers. Understanding the role of mevalonate kinase in contributing to the flux of metabolic precursors that affects such posttranslational modifications represents a potentially significant step toward the regulation of these processes.

ACKNOWLEDGMENT

We appreciate Dr. Dale Poulter's gift of farnesyl thiodiphosphate.

REFERENCES

1. Tchen, T. T. (1958) Mevalonate Kinase: Purification and Properties. *J. Biol. Chem. 233*, 1100–1103.
2. Hoffman, G., Gibson, K. M., Brandt, I. K., Bader, P. I., Wappner, R. S., and Sweetman, L. (1986) Mevalonic Aciduria: An Inborn Error of Cholesterol and Nonsterol Isoprene Biosynthesis. *N. Engl. J. Med. 314*, 1610–1614.
3. Dorsey, K. J., and Porter, J. W. (1968) The inhibition of mevalonic kinase by geranyl and farnesyl pyrophosphates. *J. Biol. Chem. 243*, 4667–4670.
4. Potter, D., and Miziorko, H. M. (1997) Identification of catalytic residues in human mevalonate kinase. *J. Biol. Chem. 272*, 25449–25454.
5. Hinson, D. D., Chambliss, K. L., Toth, M. J., Tanaka, R. D., and Gibson, K. M. (1997) Post-translational regulation of mevalonate kinase by intermediates of the cholesterol and nonsterol isoprene biosynthetic pathways. *J. Lipid Res. 38*, 2216–2223.
6. Voynova, N. E., Rios, S. E., and Miziorko, H. M. (2004) *Staphylococcus aureus* mevalonate kinase: Isolation and characterization of an enzyme of the isoprenoid biosynthetic pathway. *J. Bacteriol. 186*, 61–67.
7. Andreassi, J. L., Dabovic, K., and Leyh, T. S. (2004) *Streptococcus pneumoniae* isoprenoid biosynthesis is downregulated by diphosphomevalonate: An antimicrobial target. *Biochemistry 43*, 16461–16466.
8. Phan, R. M., and Poulter, C. D. (2001) Synthesis of (S)-isoprenoid thiodiphosphates as substrates and inhibitors. *J. Org. Chem. 66*, 6705–6710.
9. Humbelin, M., Thomas, A., Lin, J., Li, J., Jore, J., and Berry, A. (2002) Genetics of isoprenoid biosynthesis in *Paracoccus zeaxanthinifaciens*. *Gene 4*, 129–139.
10. Houten, S. M., Kuis, W., Duran, M., de Koning, T. J., van Royen-Kerkhof, A., Romeijn, G. J., Frenkel, J., Dorland, L., de Barse, M. M., Huijbers, W. A., Rijkers, G. T., Waterham, H. R., Wanders, R. J., and Poll-The, B. T. (1999) Mutations in MVK, encoding mevalonate kinase, cause hyperimmunoglobulinaemia D and periodic fever syndrome. *Nat. Genet. 22*, 175–177.
11. Fu, Z., Wang, M., Potter, D., Miziorko, H. M., and Kim, J. J. (2002) The structure of a binary complex between a mammalian mevalonate kinase and ATP: Insights into the reaction mechanism and human inherited disease. *J. Biol. Chem. 277*, 18134–18142.
12. Yang, D., Shipman, L. W., Roessner, C. A., Scott, A. I., and Sacchettini, J. C. (2002) Structure of the *Methanococcus jannaschii* mevalonate kinase, a member of the GHMP kinase superfamily. *J. Biol. Chem. 277*, 9462–9467.
13. Bork, P., Sander, C., and Valencia, A. (1993) Convergent evolution of similar enzymatic function on different protein folds: The hexokinase, ribokinase, and galactokinase families of sugar kinases. *Protein Sci. 2*, 31–40.
14. Andreassi, J., Bilder, P. W., Vetting, M. W., Roderick, S. L., and Leyh, T. S. (2007) Crystal structure of the *Streptococcus pneumoniae* mevalonate kinase in complex with diphosphomevalonate. *Protein Sci. 16*, 983–989.
15. Sgraja, T., Smith, T. K., and Hunter, W. N. (2007) Structure, substrate recognition and reactivity of *Leishmania major* mevalonate kinase. *BMC Struct. Biol.* doi: 10.1186/1472-6807-7-20.
16. Potter, D., Wojnar, J. M., Narasimhan, C., and Miziorko, H. M. (1997) Identification and Functional Characterization of an Active Site Lysine in Mevalonate Kinase. *J. Biol. Chem. 273*, 5741–5746.
17. Otwinowski, Z., and Minor, W. (1997) Processing of X-ray Diffraction Data Collected in Oscillation Mode. *Methods Enzymol. 276*, 307–326.
18. Collaborative Computational Project Number 4 (1994) The CCP4 suite: Programs for protein crystallography. *Acta Crystallogr. D50* (5), 760–763.
19. Roussel, A., Inisan, A. G., et al. (1999) *Turbo-Frodo*, version OpenGL:1, CNRS/Universitite-Marseille, Marseille, France.
20. Dundas, J., Ouyang, Z., Tseng, J., Binkowski, A., Turpaz, Y., and Liang, J. (2006) CASTp: Computed atlas of surface topography of proteins with structural and topographical mapping of functionally annotated resiudes. *Nucleic Acid Res. 34*, 116–118.
21. Houten, S. M., Wanders, R. J., and Waterham, H. R. (2000) Biochemical and genetic aspects of mevalonate kinase and its deficiency. *Biochim. Biophys. Acta 1529*, 19–32.
22. Cho, Y. K., Rios, S. E., Kim, J. J., and Miziorko, H. M. (2001) Investigation of invariant serine/threonine residues in mevalonate kinase. Tests of the functional significance of a proposed substrate binding motif and a site implicated in human inherited disease. *J. Biol. Chem. 276*, 12573–12578.
23. Park, H. W., Boduluri, S. R., Moomaw, J. F., Casey, P. J., and Beese, L. S. (1997) Crystal structure of protein farnesyltransferase at 2.25 angstrom resolution. *Science 275*, 1750–1751.
24. Tarshis, L. C., Yan, M., Poulter, C. D., and Sacchettini, J. C. (1994) Crystal structure of recombinant farnesyl diphosphate synthase at 2.6 angstrom resolution. *Biochemistry 33*, 10871–10877.
25. Lesburg, C. A., Zhai, G., Cane, D. E., and Christianson, D. W. (1997) Crystal structure of pentalenene synthase: Mechanistic insights on terpenoid cyclization reactions in biology. *Science 277*, 1820–1824.
26. Starks, C. M., Back, K., Chappell, J., and Noel, J. P. (1997) Structural basis for cyclic terpene biosynthesis by tobacco 5-epi-aristolochene synthase. *Science 277*, 1815–1820.
27. Bonanno, J. B., Edo, C., Eswar, N., Pieper, U., Romanowski, M. J., Ilyin, V., Gerchman, S. E., Kycia, H., Studier, F. W., Sali, A., and Burley, S. K. (2001) Structural genomics of enzymes involved in sterol/isoprenoid biosynthesis. *Proc. Natl. Acad. Sci. U.S.A. 98*, 12896–12901.
28. Ni, S., Robinson, H., Maarsing, G. C., Bussiere, D. E., and Kennedy, M. A. (2004) Structure of 2C-methyl-D-erithritol-2,4-cyclodiphosphate synthase from *Shewanella oneidensis* at 1.6 Å: Identification of farnesyl pyrophosphate trapped in a hydrophobic cavity. *Acta Crystallogr. D60*, 1949–1957.
29. Kemp, L. E., Alphey, M. S., Bond, C. S., Ferguson, M. A. J., Hecht, S., Bacher, A., Eisenreich, W., Rohdich, F., and Hunter, W. N.

(2005) The identification of isoprenoids that bind in the intersubunit cavity of Escherichia coli 2C-methyl-D-erthyritol-2,4-cyclopdiphosphate synthase by complementary biophysical methods. *Acta Cryst. D61* 45–52.

30. Kraulis, J. (1991) MOLSCRIPT: A program to produce both detailed and schematic plots of protein structures. *J. Appl. Crystallogr. 24*, 946–950.
31. Merritt, E. A., and Murphy, M. E. P. (1994) Raster3D. *Acta Crystallogr. D50*, 869–873.
32. Barton, G. J. (1993) ALSCRIPT: A tool to format multiple sequence alignments. *Protein Eng. 6* (1), 37–40.
33. DeLano, W. L. (2002) *The PyMOL Molecular Graphics System*, DeLano Scientific, Palo Alto, CA.

BI7024386